Electronic Supplementary Material (ESI) for Journal of Materials Chemistry A.

The Relationship between Coefficient of Restitution and State of Charge of Zinc Alkaline Primary LR6 Batteries

Shoham Bhadra,[a] Benjamin J. Hertzberg,[b] Andrew Hsieh,[b] Mark Croft,[c] Joshua W. Gallaway,[d] Barry J. Van Tassell,[e] Mylad Chamoun,[f] Can Erdonmez,[f] Zhong Zhong,[g], Tal Sholklapper,[h] and Daniel A. Steingart[*b]

[a] *Electrical Engineering and the Andlinger Center for Energy and the Environment, Princeton University, Princeton, New Jersey 08540, USA.*

[b] *Mechanical and Aerospace Engineering and the Andlinger Center for Energy and the Environment, Princeton University,Princeton, New Jersey 08540, USA.*

[c] *Department of Physics, Rutgers University, Piscataway, New Jersey 08854, USA.*

[d] *City University of New York Energy Institute, New York, New York 10031, USA.*

[e] *Department of Chemical Engineering, City College of New York, New York, New York 10031, USA.*

[f] *Sustainable Technologies Division, Brookhaven National Laboratory, Upton, New York 11973, USA.*

[g] *National Synchrotron Light Source, Brookhaven National Laboratory, Upton, New York 11973, USA.*

[*] **Direct correspondence to: steingart@princeton.edu**

1 Methods

Materials
The batteries used were Duracell Coppertop LR6 batteries with a nominal initial voltage of 1.65 V, and a nominal capacity of 2850 mAh. Prior to testing, a representative LR6 cell was dismantled and the individual parts weighed to determine component mass. Weighing was done using a Metler-Toledo lab balance accurate to 0.1 mg. Components were then dried at 25C under vacuum for 48 hours in a VWR Symphony vacuum oven, after which components were again weighed to determine system mass after dehydration.
Batteries were discharged at a rate of C/10 (280 mA) using a Neware BT3000-8 cycler for one hour intervals followed by a 15 minute rest period at open-circuit conditions, prior to performing electrochemical impedance spectroscopy and drop testing. Following every discharge cycle, batteries were weighed.

Electrochemical impedance spectroscopy
Electrochemical impedance spectroscopy was performed on each cell using a Gamry Reference 3000 unit after every 280 mAhr of capacity discharge. Scans were performed under potentiostatic conditions at the open circuit voltage of each cell, with an AC voltage perturbation of 10 mV, sweeping from 100 mHz to 100 kHz.

Bounce tests
Batteries were dropped 25 cm through an acrylic tube of 18 mm diameter onto an epoxy bench top. The usage of the acrylic tube ensured equivalence of each drop test. The audio profile of each drop was recorded using a microphone placed 30 cm away, and later analyzed using a python script to determine number of bounces, height of bounce, and coefficient of restitution.

X-ray diffraction
In situ XRD was done at Beamline X17B1 of the National Synchrotron Light Sources (NSLS) at Brookhaven National Lab. Beamline X17B1 is an energy dispersive x-ray line capable of measuring internal structural changes in a discrete volume. LR6 form factor batteries were analyzed using methodology that has been described in detail by Gallaway et al.

2 Supplemental figures

Supp. Figure 1. Schematic of bounce test setup. Bounce tests were performed by dropping alkaline AA batteries through a clear acrylic tube from a height of 25 cm. The audio produced by the bouncing was recorded using a microphone and a laptop computer.

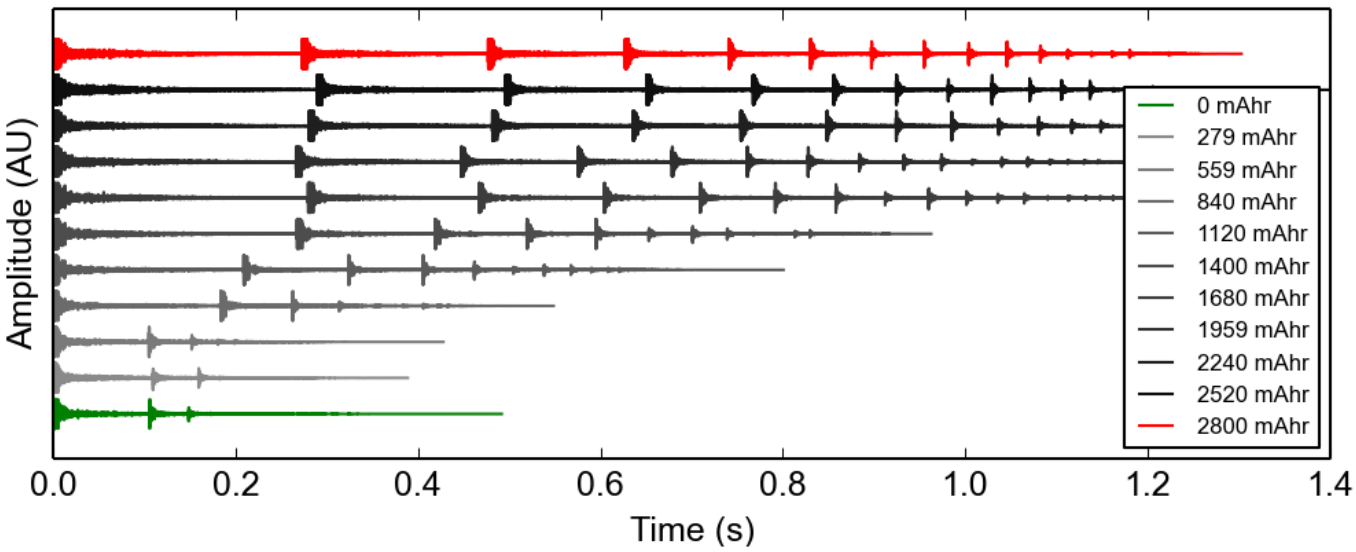

Supp. Figure 2. Bounce audio waveform evolution during discharge. The increase in COR is evident by viewing the increase in time between the first and second bounces. The saturation is also clear after 50% SOC is reached, though the batteries appear to continue to bounce for longer periods even after saturation of COR.

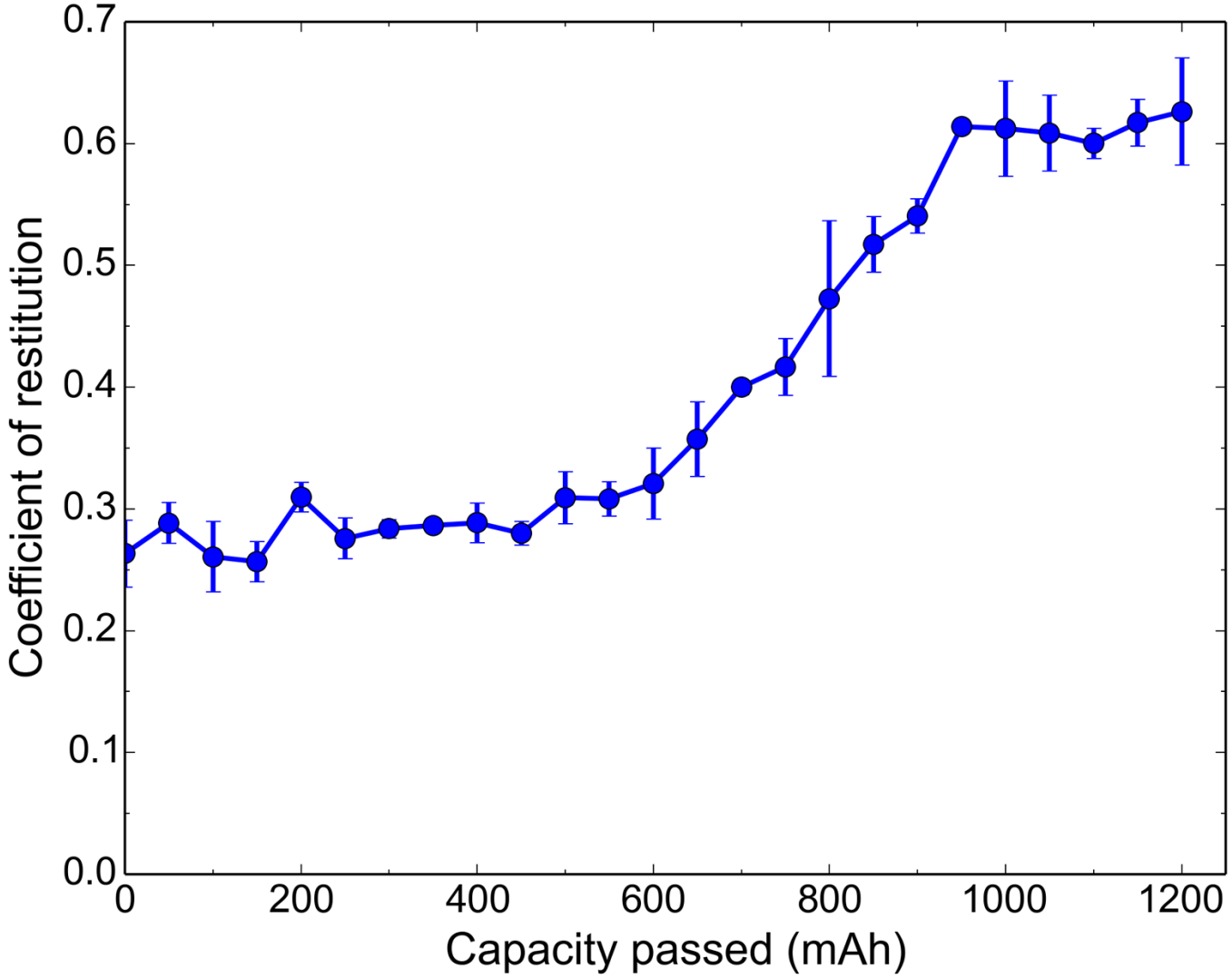

Supp. Figure 3. (color online) Coefficient of restitution as a function of capacity passed at 50 mA in 50 mAh increments, showing the increase in coefficient of restitution at 450 mAh passed, and saturation at 950 mAh passed.

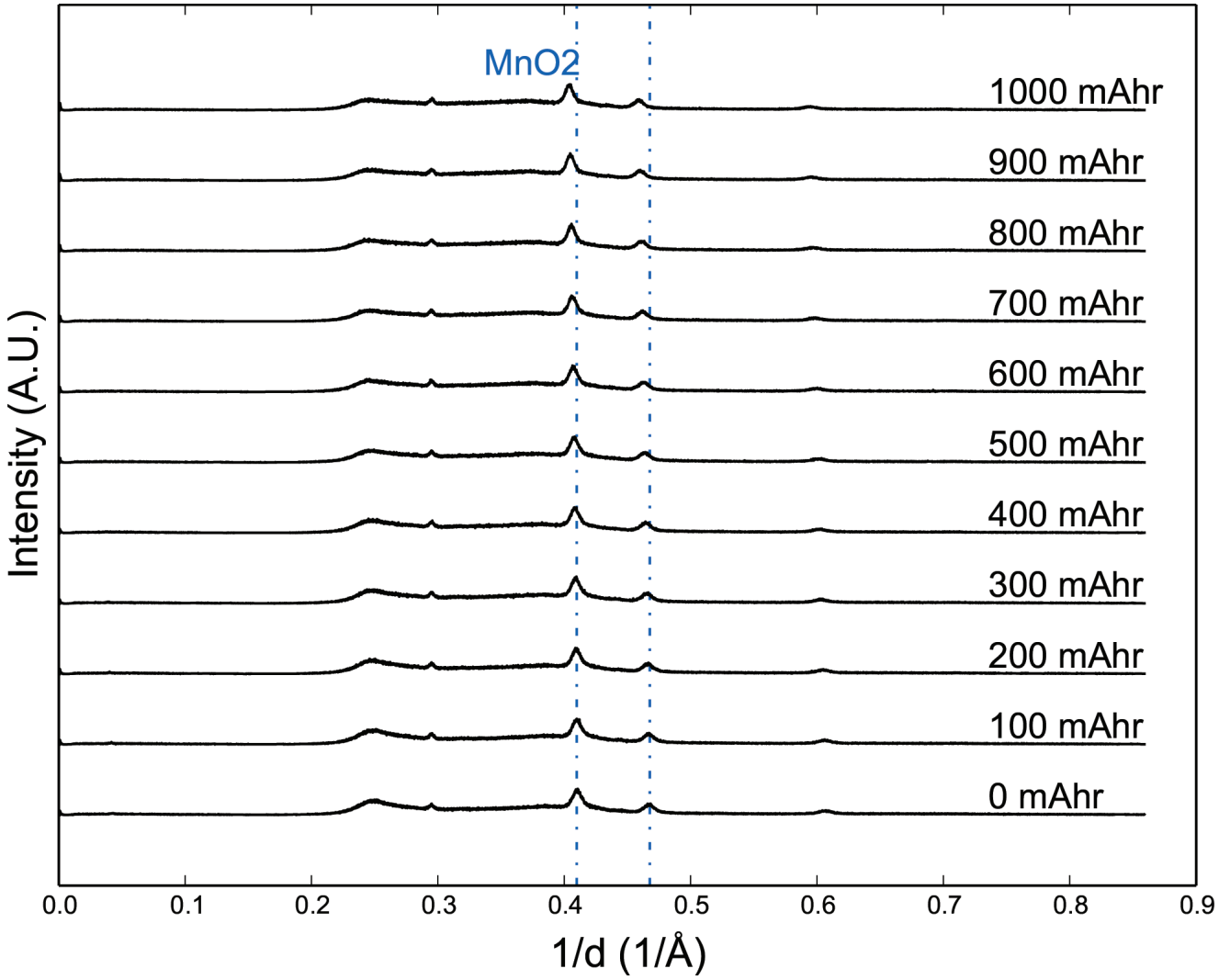

Supp. Figure 4. Representative MnO_2 EDXRD spectra at 100 mA discharge rate. A continuous shift of the MnO_2 peaks is clear starting at 100 mAh of charge passed.

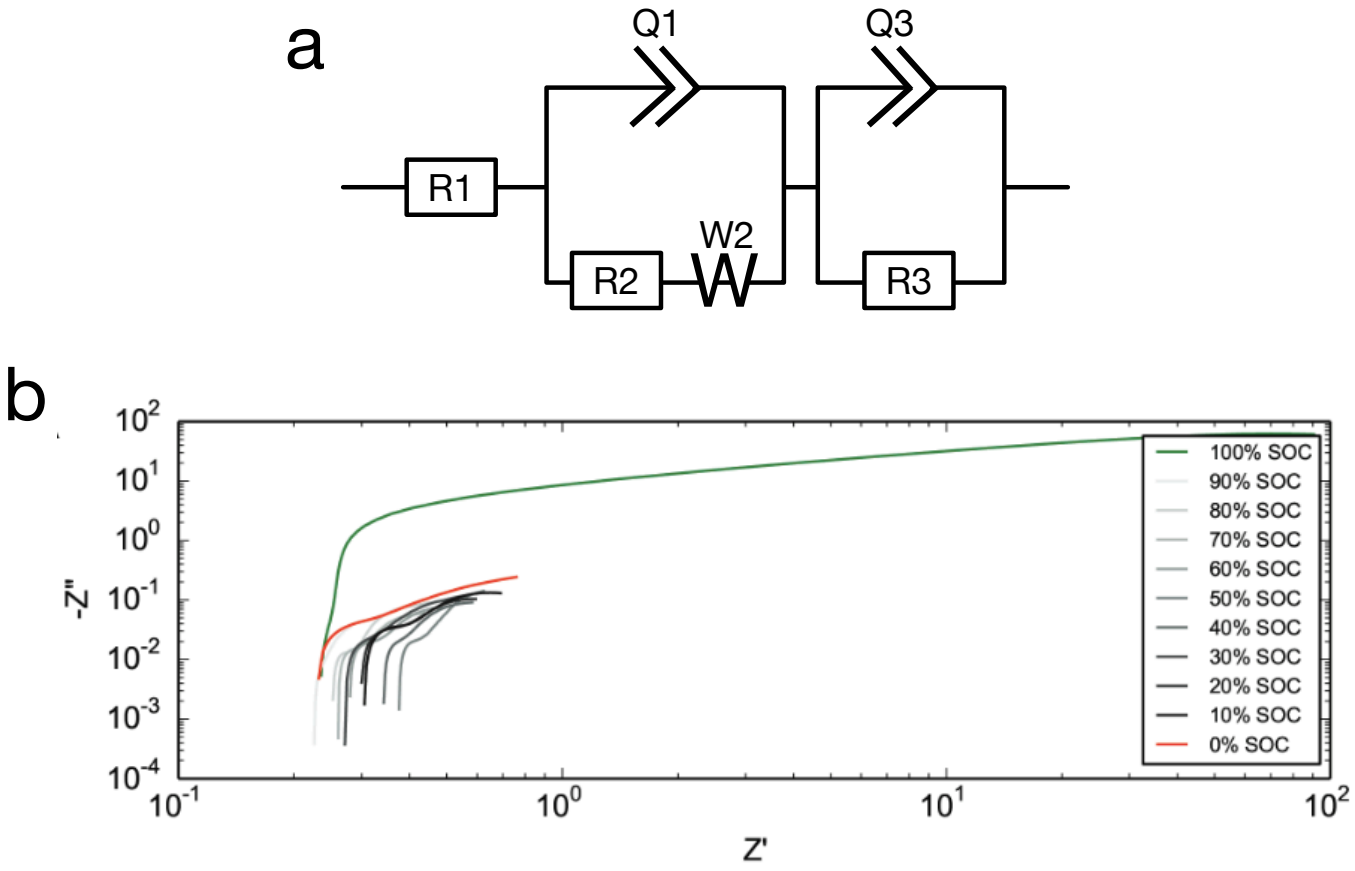

Supp. Figure 5. (color online). a) Circuit diagram of EIS model used; b) Nyquist impedance plot for a representative cell, measured from as-received (green) to fully-discharged (red). Scans performed from 100 mHz to 100 kHz. Our results in Supp. Fig. 5b agree with previous impedance spectroscopy experiments on alkaline LR6-type cells.[1,2] In the Nyquist plots, High reactance (Z") and resistance (Z') are visible in the as received cell, with a two order of magnitude drop in both following 10% discharge of the cell. A maximum in solution resistance occurs at 50% SOC. Reactance remains constant. Our tests of our system show that it can be modeled with a standard Randles circuit, modified by the addition of a second phase with separate charge-transfer and double-layer capacitance impedance values. This model is shown in Supp. Figure 5a. Over time, the Ohmic impedance of the system, typically dominated by the ionic impedance of the electrolyte, stays roughly constant with State-of-Charge (SOC), up until 50% SOC, when a significant spike in Ohmic impedance occurs. This increase correlates with the leveling of the coefficient-of-restitution changes caused by the transition between the formation of Type I ZnO to Type II ZnO. The double-layer capacitance of both phases present decreases with decreasing state-of-charge. This suggests that there is a continuous decrease in the total surface area of the available Zn anode with cycling, which correlates well with the phase transformation from Zn to ZnO, as ZnO is less dense than Zn . This is in strong agreement with Haibel, Manke and Gallaway.[3–5] What we see is a complex mix within the impedance data, where increasing impedance throughout the entire discharge is attributed to 1) loss of solvent (consumption of water) in the protonation of MnO_2 and the oxidation of Zn, 2) ZnO formation which passivates and blocks the Zn surface, and 3) Increasing concentration of alkaline salts in the remaining water which decreases the conductivity of the electrolyte above.[6]

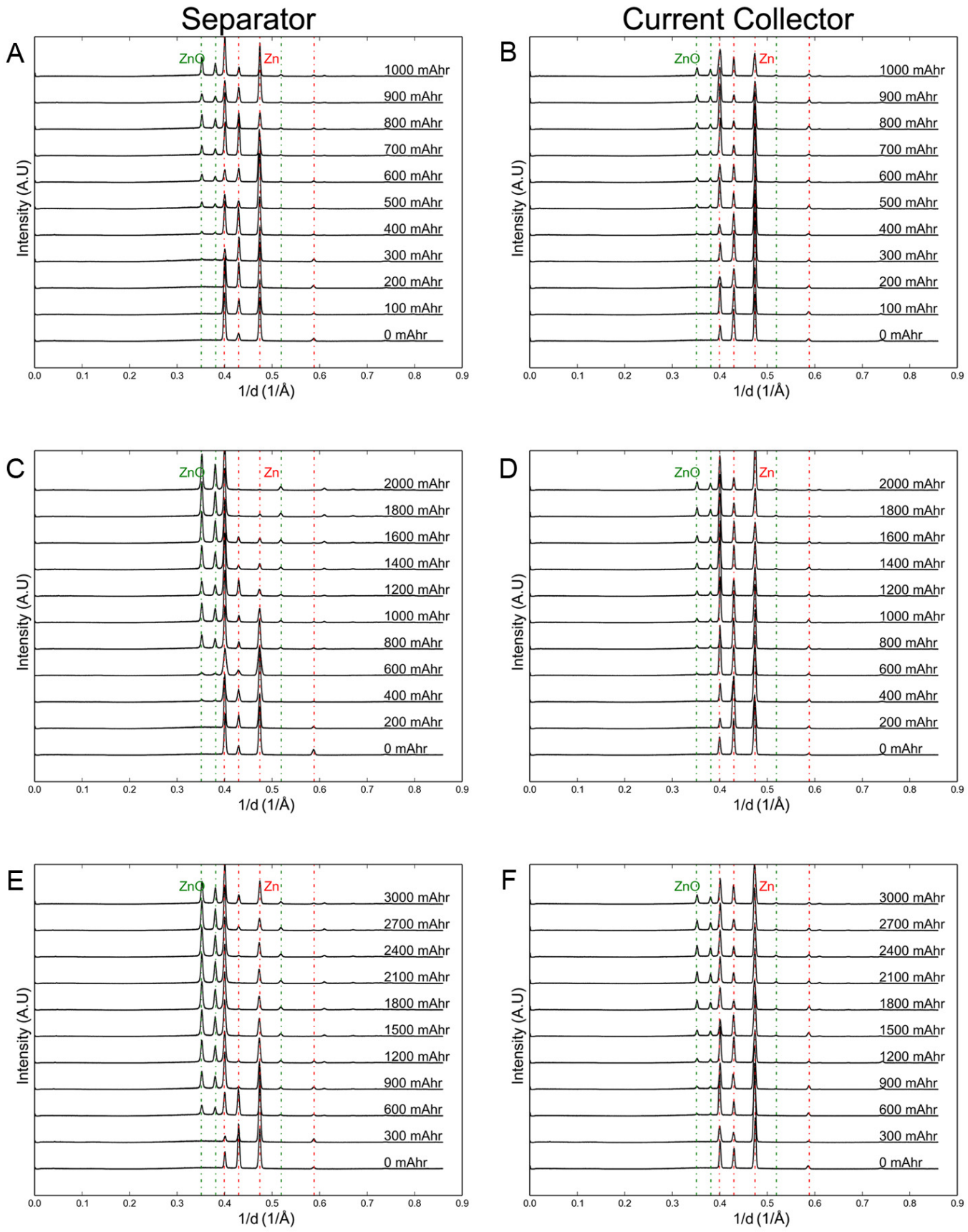

Supp. Figure 6. (color online). XRD progression of anode at separator and current collector interfaces at a,b) 100 mA, c,d) 200 mA, and e,f) 300 mA. ZnO peaks are denoted by green dashed lines, and Zn peaks are denoted by red dashed lines. In all cases, ZnO forms at the separator before forming at the current collector.

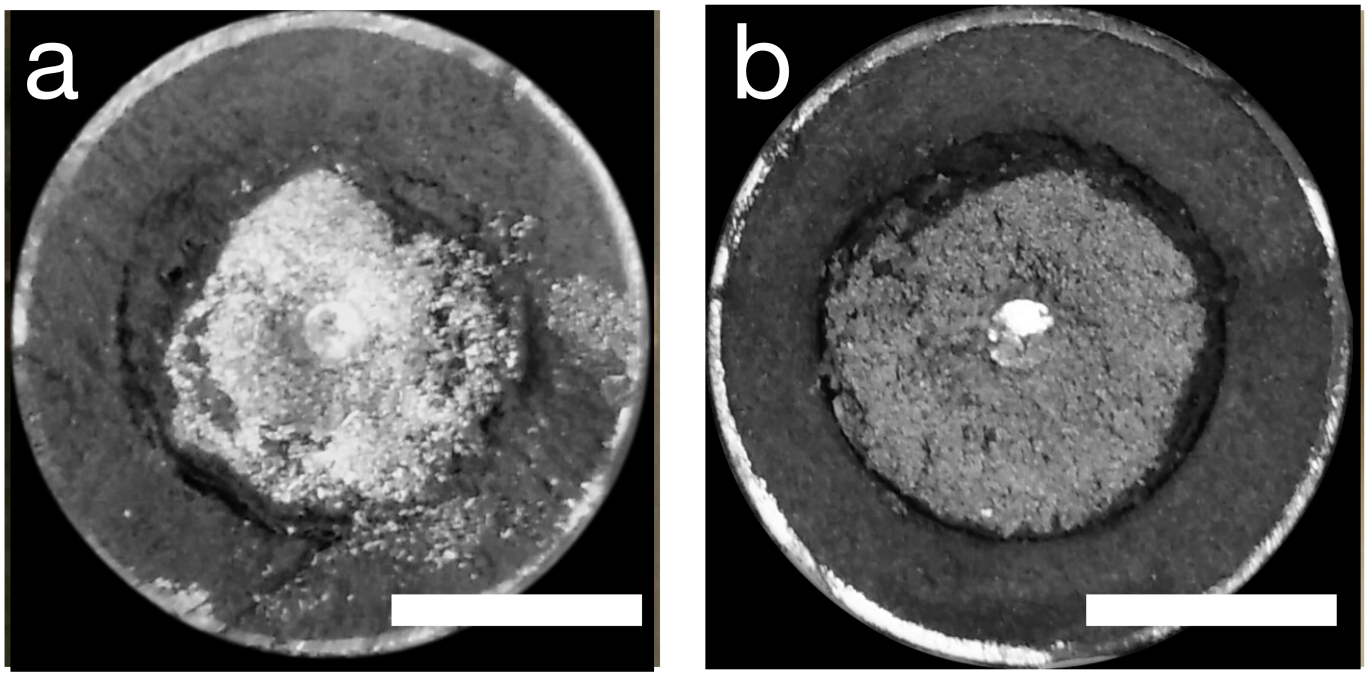

Supp. Figure 7. Comparison of a) a fresh alkaline LR6 cell and b) a dessicated alkaline LR6 cell. The anode of the fresh cell has a shiny, paste-like consistency, while the anode of the dessicated cell has a darker, more granular consistency. Mechanically, the fresh anode behaves like a viscous paste, the dessicated anode behaves like a pasty, granular mass. . Scale bar = 5 mm

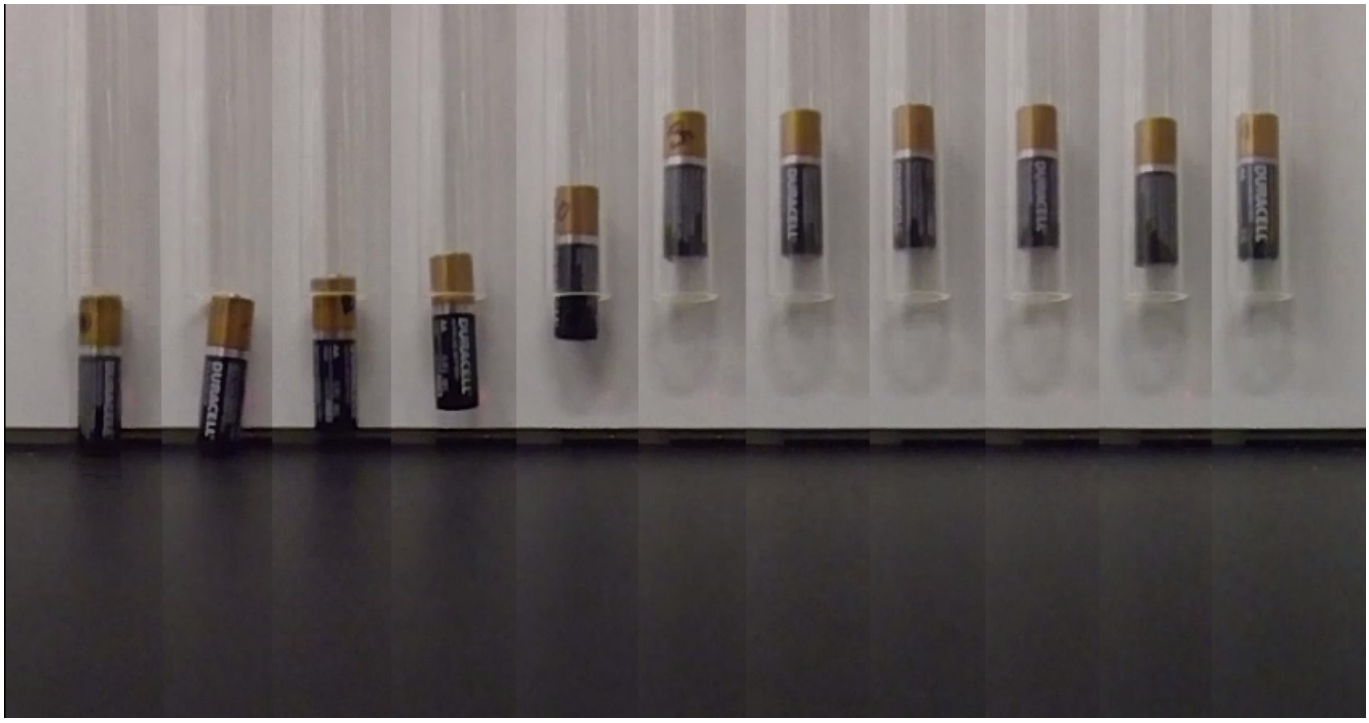

Supp. Movie 1. Composited footage of a single AA alkaline cell at 11 depths of discharge showing the increase and saturation of bounce height. Video also available online at
<http://drops.steingart.princeton.edu/static/realfiles/BouncingBatteries/SuppMovie1.mp4>

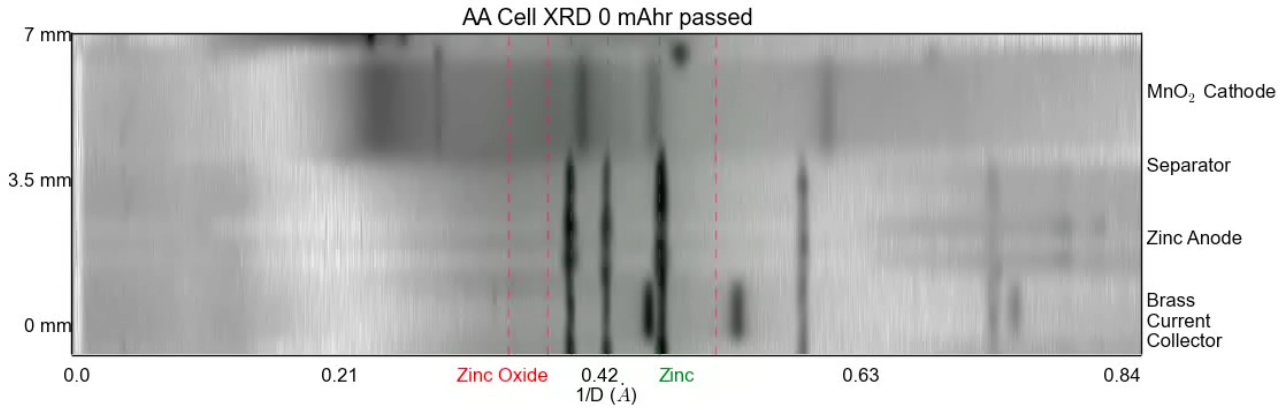

Supp. Movie 2. A timelapse EDXRD (1 frame per hour) showing the complete change in structure of the AA battery during a 200 mA discharge. Note the progression of ZnO from separator to current collector and the eventual depletion of Zn at the separator surface. Video also available online at
<http://drops.steingart.princeton.edu/static/realfiles/BouncingBatteries/SuppMovie2.mp4>

References

[1] J. M. Wang, Y. D. Qian, J. Q. Zhang and C. N. Cao, *J. Appl. Electrochem.*, 2000, 30, 113–116.

[2] M. Root, *J. Appl. Electrochem.*, 1995, 25, 1057–1060.

[3] A. Haibel, I. Manke, A. Melzer and J. Banhart, *J. Electrochem. Soc.*, 2010, 157, A387–A391.

[4] I. Manke, J. Banhart, A. Haibel, A. Rack, S. Zabler, N. Kardjilov, A. Hilger, A. Melzer and H. Riesemeier, *Appl. Phys. Lett.*, 2007, 90, 214102.

[5] J. W. Gallaway, C. K. Erdonmez, Z. Zhong, M. Croft, L. A. Sviridov, T. Z. Sholklapper, D. E. Turney, S. Banerjee and D. A. Steingart, *J. Mater. Chem. A*, 2014, 2, 2757–2764.

[6] T. Reddy, *Linden's Handbook of Batteries, 4th Edition*, McGraw-Hill Education, 2010.